

Chirality effects in carbon nanotubes.

E.L. Ivchenko

A.F.Ioffe Physical-Technical Institute, 194021 St. Petersburg, Russia

B. Spivak

Physics Department, University of Washington, Seattle, WA 98195, USA

Abstract

We consider chirality related effects in optical, photogalvanic and electron-transport properties of carbon nanotubes. We show that these properties of chiral nanotubes are determined by terms in the electron effective Hamiltonian describing the coupling between the electron wavevector along the tube principal axis and the orbital momentum around the tube circumference. We develop a theory of photogalvanic effects and a theory of *dc* electric current, which is linear in the magnetic field and quadratic in the bias voltage. Moreover, we present analytic estimations for the natural circular dichroism and magneto-spatial effect in the light absorption.

PACS: 05.20-y, 82.20-w

I. INTRODUCTION

Since the discovery of carbon nanotubes [1] the physical properties of these nanostructures have attracted a lot of attention [2]. Usually carbon nanotubes (CNs) are visualized as a layer of graphene sheet rolled-up into a cylinder. Depending of the way of the rolling up the cylinder can be chiral or non-chiral.

In media with chiral symmetry it is impossible to distinguish between polar and axial vectors. This leads to the existence of the natural optical activity [3], including the optical rotatory power and circular dichroism in the absence of magnetic fields, and any other effect of chirality where a polar vector and an axial vector (or a pseudovector) are interrelated by some phenomenological equation. The circular photogalvanic effect (CPGE) is among them. In this effect a *dc* current induced by an electro-magnetic wave of the complex amplitude \mathbf{E} is proportional to components of the axial vector $i(\mathbf{E} \times \mathbf{E}^*)$ and thus depends on the sign of the circular polarization of light. The CPGE was predicted in [4,5] and then studied in bulk gyrotropic crystals [6,7] and semiconductor quantum-well structures [8–10].

Theoretically, achiral magnetic properties and optical absorption spectra of CNs were investigated by Ajiki and Ando in the effective-mass approximation [11–13] (see also [14]). The theory of the optical activity of CNs has been considered by Tasaki et al. [3] in the framework of the microscopic tight-binding model.

In the present paper we consider effects of chirality in CNs by extending the effective-mass theory [11–13]. We show that these effects appear due to terms in the electron Hamiltonian describing the coupling between the orbital momentum around the circumference of a chiral CN and the linear electron momentum along the tube. This is quite different from the case of bulk materials and semiconductor quantum wells where these effects are attributed to spin-orbit terms $\sigma_\alpha k_\beta$ in the electron effective Hamiltonian (σ_α and \mathbf{k} are the Pauli spin matrices and the electron wave vector; α, β are the cartesian coordinates) [4,10] (see also [18]).

The paper is organized as follows. In Sec. II we briefly review properties of the single

particle electron spectrum of CNs and derive an expression for the matrix element of the electron-photon interaction. In Secs. III and IV we present the theory of photogalvanic effects in chiral CNs. We show that the circularly polarized light generates a *dc* current through CN and the current direction depends on the sign of polarization, i.e. on the photon spirality. In the presence of an external magnetic field B parallel to the nanotube principal axis, the linearly polarized light generates a *dc* current whose direction changes upon the inversion of B . In Sec. V we develop a theory of the magneto-chiral anisotropy in the *dc* charge transport through a CN, which is the existence of a *dc* current proportional to B and quadratic in the applied electric field E . In Sec. VI we give analytical estimates for the optical anisotropy and optical activity of CN. In Sec. VII we discuss limitations of our approach and mention other effects which are similar to those considered in this article.

II. ELECTRON BAND STRUCTURE AND ELECTRON-PHOTON MATRIX ELEMENTS IN CARBON NANOTUBES.

Usually carbon nanotubes (CNs) are visualized as a conformal mapping of a graphene sheet onto a cylindrical surface where one of the two-dimensional (2D) Bravais lattice vectors, \mathbf{L} , maps to the cylinder circumference [15–17]. The structures specified by the vectors \mathbf{L} directed along one of the two-fold rotation axes u_2 or u'_2 are called respectively armchair and zigzag CNs, where the axis u_2 is parallel and the axis u'_2 is perpendicular at least to one side of the 2D lattice hexagon. These particular tubes are achiral. Except for them all others are chiral with their principal axis z being the screw axis.

Following [11–13] we write the circumferential vector as

$$\mathbf{L} = n_a \mathbf{a} + n_b \mathbf{b}, \quad (1)$$

where n_a, n_b are integers and \mathbf{a}, \mathbf{b} are the 2D basis vectors with the angle 120° between them. Choosing the coordinate system x_1, x_2 in such a way that $x_1 \parallel \mathbf{a}$, $x_2 \perp \mathbf{a}$ we have for the components of \mathbf{a} and \mathbf{b}

$$\mathbf{a} = a(1, 0), \mathbf{b} = a \left(-\frac{1}{2}, \frac{\sqrt{3}}{2} \right), \quad (2)$$

where the lattice constant a is equal to $\sqrt{3}$ times the interatomic distance $d = 1.44 \text{ \AA}$ [19].

The electron effective Hamiltonian for a graphene sheet,

$$H = \begin{pmatrix} 0 & h^* \\ h & 0 \end{pmatrix}, \quad (3)$$

is expanded in the vicinity of the points

$$\mathbf{K} = \frac{4\pi}{3a}(-1, 0), \mathbf{K}' = \frac{4\pi}{3a}(1, 0) \quad (4)$$

at the corners of the 2D Brillouin zone shown in Fig. 1. In the following we define \mathbf{k} and \mathbf{k}' as wavevectors referred respectively to the points \mathbf{K} and \mathbf{K}' and assume the products $ka, k'a \ll 1$ to be small. Then, in the second order in ka or $k'a$, the matrix element h in Eq. (3) is given by (see [13])

$$h(\mathbf{k}, \mathbf{K}) = \gamma e^{-i\theta} \left[k_{\perp} - ik_z + \frac{a}{4\sqrt{3}} e^{3i\theta} (k_{\perp} + ik_z)^2 \right] \quad (5)$$

near the \mathbf{K} point and

$$h(\mathbf{k}', \mathbf{K}') = \gamma e^{i\theta} \left[-k'_{\perp} - ik'_z + \frac{a}{4\sqrt{3}} e^{-3i\theta} (k'_{\perp} - ik'_z)^2 \right] \quad (6)$$

near the \mathbf{K}' point. Here $\gamma = \frac{\sqrt{3}}{2}\gamma_0 a$, γ_0 ($\approx 3 \text{ eV}$ [11,19]) is the transfer integral between neighboring π orbitals, θ is the angle between the vector \mathbf{L} and the basis vector \mathbf{a} . The subscripts z, \perp indicate components of a vector referred to the axes lying in the graphene plane and related to the vector \mathbf{L} so as $z \perp \mathbf{L}$ and $k_z \perp \mathbf{L}$, $k_{\perp} \parallel \mathbf{L}$.

In the same approximation the energy spectrum near the \mathbf{K} point is given by

$$E_{c,v}(\mathbf{k}, \mathbf{K}) = \pm |h| \approx \pm \gamma \left\{ |\mathbf{k}| + \frac{a}{4\sqrt{3}|\mathbf{k}|} \left[(k_{\perp}^3 - 3k_{\perp}k_z^2) \cos 3\theta + (k_z^3 - 3k_{\perp}^2k_z) \sin 3\theta \right] \right\}, \quad (7)$$

where $|\mathbf{k}| = \sqrt{k_{\perp}^2 + k_z^2}$, the upper and lower signs represent the conduction (subscript c) and valence (subscript v) bands respectively. The similar spectrum near the \mathbf{K}' point is obtained

by changing $k_{\perp} \rightarrow -k'_{\perp}$, $k_z \rightarrow k'_z$, $\theta \rightarrow -\theta$ in agreement with the time inversion symmetry requirement $E_{c,v}(\mathbf{k}, \mathbf{K}') = E_{c,v}(-\mathbf{k}, \mathbf{K})$.

In a CN specified by the vector \mathbf{L} the electron wave function satisfies the cyclic boundary condition $\Psi(\mathbf{r}) = \Psi(\mathbf{r} + \mathbf{L})$. This enables one to find the allowed discrete values of k_{\perp} as

$$k_{\perp} = \frac{2\pi}{L} \left(n - \frac{\nu}{3} \right) ; k'_{\perp} = \frac{2\pi}{L} \left(n + \frac{\nu}{3} \right), \quad (8)$$

where n is an integer $0, \pm 1, \pm 2, \dots$ characterizing the angular momentum component of an electron, $L = |\mathbf{L}| = a\sqrt{n_a^2 + n_b^2 - n_a n_b}$, and ν equals to one of three integers: $0, \pm 1$ determined by the presentation of the sum $n_a + n_b$ as $3N + \nu$ with integer N . The dispersion in the conduction and valence subbands is obtained by substituting Eq. (8) into Eqs. (5,6) or Eq. (7). In the following we focus on the nanotubes characterized by finite band gap and assume $\nu \neq 0$. According to Eq. (7), for small values of k_z satisfying the condition $|k_z| \ll |k_{\perp}|$ in the K valley and similar condition in the K' valley, the electron spectrum has a parabolic form with terms linear in k_z

$$E_{c,v}(n, k_z; K) = \pm \left(\frac{\Delta_n}{2} + \frac{\hbar^2 k_z^2}{2m_n} + \beta_n k_z \right), \quad (9)$$

$$E_{c,v}(n, k'_z; K') = \pm \left(\frac{\Delta'_n}{2} + \frac{\hbar^2 k_z'^2}{2m'_n} + \beta'_n k'_z \right),$$

where

$$\Delta_n = 2\gamma|k_{\perp}|, \quad \Delta'_n = 2\gamma|k'_{\perp}|, \quad (10)$$

$$m_n = \frac{\hbar^2|k_{\perp}|}{\gamma}, \quad m'_n = \frac{\hbar^2|k'_{\perp}|}{\gamma}, \quad (11)$$

$$\beta_n = -\frac{\sqrt{3}}{4}\gamma a|k_{\perp}| \sin 3\theta, \quad \beta'_n = \frac{\sqrt{3}}{4}\gamma a|k'_{\perp}| \sin 3\theta, \quad (12)$$

and k_{\perp}, k'_{\perp} are defined in Eq. (8). Note that the identity $E_{c,v}(n, k_z; K') = E_{c,v}(-n, -k_z; K)$ follows directly from the time inversion symmetry.

In the presence of an external magnetic field \mathbf{B} , the electron energy is modified just by changing k_{\perp}, k'_{\perp} from Eq. (8) into

$$k_{\perp} = \frac{2\pi}{L} \left(n - \frac{\nu}{3} + \frac{\Phi}{\Phi_0} \right) ; k'_{\perp} = \frac{2\pi}{L} \left(n + \frac{\nu}{3} + \frac{\Phi}{\Phi_0} \right) , \quad (13)$$

where Φ is the magnetic flux passing through the cross section of a CN, $\Phi = B_z L^2 / (4\pi)$, and Φ_0 is the magnetic flux quantum, ch/e . Now the consequence of the time inversion symmetry takes the form $E_{c,v}(n, k_z; \Phi; K') = E_{c,v}(-n, -k_z; -\Phi; K)$.

Chirality (or spirality) of a nanotube manifests itself in a particular coupling between the angular momentum as described by n and the directed translational motion as described by k_z : due to the terms linear- k_z in Eq. (9) or, in general, due to odd-in- k_z terms in Eq. (7) the energy has a contribution which depends both on the *sign* of k_z and the *sign* of n .

It is interesting to analyze how this particular coupling disappears for zigzag and armchair tubes which are achiral from the symmetry point of view. In zigzag tubes, the angle θ between the circumferential vector \mathbf{L} and the vector \mathbf{a} is an integer multiple of 60° , $\sin 3\theta$ is zero and odd-in- k_z terms in Eqs. (7,9) vanish. In armchair tubes, the angle θ equals to $\theta = 30^\circ + N \cdot 60^\circ$ with N integer leading to one of the following three relations between n_a and n_b : $n_a = 2n_b$ or $n_b = 2n_a$ or $n_b = -n_a$. This means that the sum $n_a + n_b$ is an integer multiple of 3 and the parameter ν is zero. As a result values of $|k_{\perp}|$ become independent of the sign of n and the coupling between signs of n and k_z in the terms odd-in- k_z terms. This follows also from the symmetry considerations and is an important check point. In the following sections we will show that the odd-in- k_z terms in the electron energy spectrum govern the chirality effects in CNs.

Let us now turn to the calculation of the matrix element, V_{fi} , for the electron optical transition between the initial state i and the final state f . The electron envelope functions can be written in the form

$$\psi_{c,v}(z; n, k_z) = \frac{e^{in\varphi}}{\sqrt{2\pi}} \frac{e^{ik_z z}}{\sqrt{L_{CN}}} \hat{C}_{c,v}(n, k_z) , \quad (14)$$

where L_{CN} is the nanotube length and φ is the azimuth angle. The two-component columns $\hat{C}_{c,v}$ are eigenvectors of the 2×2 matrix Hamiltonian (3), given by

$$\hat{C}_c = \frac{1}{\sqrt{2}} \begin{bmatrix} h^*/|h| \\ 1 \end{bmatrix}, \quad \hat{C}_v = \frac{1}{\sqrt{2}} \begin{bmatrix} 1 \\ -h/|h| \end{bmatrix} \quad (15)$$

with h defined by Eq. (5) for the K valley and by Eq. (6) for the K' valley where K, K' are the z -components of the vectors \mathbf{K}, \mathbf{K}' .

We remind that the electron interaction with the electromagnetic field is described by the perturbation $(e/c)\{\hat{\mathbf{v}}\mathbf{A}\}_s$, where \mathbf{A} is the vector potential of the field, $-e$ is the electron charge, $\hat{\mathbf{v}}$ is the electron velocity operator $\hbar^{-1}dH/dk_z$ and the symbol $\{\dots\}_s$ means a symmetrized product of operators. If $|k_z| \ll |k_\perp|$ then one can neglect the second-order terms in the expansion Eq.(5), the symmetrization symbol can be omitted and the scalar product of $\hat{\mathbf{v}}$ and the light unit polarization vector \mathbf{e} has the form

$$\hat{\mathbf{v}} \cdot \mathbf{e} = \frac{i\gamma}{2\hbar} \begin{bmatrix} 0 & e^{i\theta} f_{12} \\ e^{-i\theta} f_{21} & 0 \end{bmatrix}. \quad (16)$$

Here

$$f_{12} = e^{i\varphi} e_- - e^{-i\varphi} e_+ + e_z, \quad f_{21} = e^{i\varphi} e_- - e^{-i\varphi} e_+ - e_z,$$

$e_\pm = e_x \pm ie_y$ and x, y are rectangular axes perpendicular to the principal axis z of the tube. The selection rules for matrix elements of the operator taken between the envelope functions Eq.(16) are in agreement with the conservation law for z -components of the angular momenta: $n_f = n_i + n_{phot}$, where $n_{phot} = \pm 1$ for the circular polarization σ_\pm of a photon propagating along the z axis and $n_{phot} = 0$ for the light linearly polarized along z . In particular, the transitions $(c, 0, K) \rightarrow (c, 1, K)$, $(c, 0, K') \rightarrow (c, -1, K')$ occur respectively under the σ_+ and σ_- photoexcitation. The squared moduli of the corresponding matrix elements are given by

$$|(\hat{\mathbf{v}} \cdot \mathbf{e})_{fi}|^2 = \frac{1}{8} \left[\frac{\gamma}{\hbar} k_z \left(\frac{1}{k_{\perp,0}} - \frac{1}{k_{\perp,1}} \right) \right]^2 = \frac{1}{32} \left(\frac{\gamma}{\hbar} \frac{k_z}{k_{\perp,0}} \right)^2, \quad (17)$$

where we took into account that $k_{\perp,1} = 2k_{\perp,0}$. The transitions under consideration are forbidden at the \mathbf{K} and \mathbf{K}' points but become allowed for $k_z, k'_z \neq 0$. The squared moduli of the optical matrix element is given by

$$|V_{fi}|^2 = \left(\frac{e}{c}A\right)^2 |(\hat{\mathbf{v}} \cdot \mathbf{e})_{fi}|^2 = \frac{2\pi e^2 I}{\omega^2 c n_\omega} \frac{1}{32} \left(\frac{\gamma}{\hbar} \frac{k_z}{k_{\perp,0}}\right)^2, \quad (18)$$

where $A = |\mathbf{A}|$, I is the light intensity and n_ω is the refractive index of the medium. In the following we consider a free-standing nanotube and assume $n_\omega = 1$.

It should be stressed that the linear-optics approximation is valid as long as $\hbar^{-1}|V_{fi}| \ll (2\tau_p)^{-1}$, otherwise one has to take into account the saturation of the absorption. Another important point is that the depolarization effect [3,12] can be neglected provided

$$\left|\frac{4\pi\sigma_\perp}{L\omega}\right| \ll 1, \quad (19)$$

where σ_\perp is the conductivity at the frequency ω defined as

$$\hbar\omega W = 2\sigma_\perp \left(\frac{\omega}{c}A\right)^2$$

with W being the optical transition rate.

III. CIRCULAR PHOTOGALVANIC EFFECT

Physically, the CPGE can be considered as a transformation of the photon angular momenta into a translational motion of free charge carriers. It is an electron analog of mechanical systems which transmit rotatory motion to linear one like a screw tread or a plane with a propeller. Phenomenologically, in the case of chiral CNs it is described by

$$j_{CPGE,z} = \Gamma i(\mathbf{E} \times \mathbf{E}^*)_z, \quad (20)$$

where $j_{CPGE,z}$ is the *dc* photocurrent, Γ is a real coefficient, \mathbf{E} is the complex amplitude of the electric field of the electromagnetic wave and, for the transverse wave,

$$i(\mathbf{E} \times \mathbf{E}^*) = P_{circ} E_0^2 \hat{o} \quad (21)$$

with E_0 , P_{circ} , \hat{o} being respectively the electric field amplitude $|\mathbf{E}|$, the degree of the circular polarization of light and the unit vector pointing in the direction of light propagation. The

photocurrent (20) reverses its direction under inversion of the light circular polarization and vanishes for linearly-polarized excitation.

Usually the microscopic theory of natural optical activity in bulk semiconductors [18,20] as well as the theory of CPGE [4,10] is based on allowance of spin-dependent linear in \mathbf{k} terms $\beta_{lm}\sigma_l k_m$ in the electron effective Hamiltonian, where \mathbf{k} is the electron wavevector and σ_l are the Pauli spin matrices. The real coefficients β_{lm} form a pseudotensor subjected to the same symmetry restriction as the pseudotensors describing the optical activity and CPGE. In CNs the spin-orbit interaction is negligible and the similar role is played by the coupling between the orbital angular momentum n and the wave vector k_z as described by Eqs. (7,9).

The transfer of photon angular momenta into an electric current along the principal axis of a chiral CN can be described by the standard equation for the current

$$j_{CPGE,z} = -e \sum_{n,k_z,s} v_c(n, k_z, s) f_c(n, k_z, s) + e \sum_{n,k_z,s} v_h(n, k_z, s) f_h(n, k_z, s), \quad (22)$$

where e is the elementary charge ($e > 0$), the index s labels the valleys K and K' , $v_c(n, k_z, s) = \hbar^{-1}(dE_c(n, k_z, s)/dk_z)$ is the group velocity and $f_c(n, k_z, s)$ is the nonequilibrium steady-state distribution function for electrons in the conduction band. The similar quantities for holes in the valence band v have the subscript h . Note that they are related with the corresponding quantities in the electron representation of the valence states by $v_h(n, k_z, K) = -v_v(-n, -k_z, K')$, $f_h(n, k_z, K) = 1 - f_v(-n, -k_z, K')$.

In the following we will consider the case where elastic scattering processes are more effective than the inelastic ones. Then one can apply the standard procedure of solving the kinetic equation and decompose the distribution function f_m ($m = c, h$) into the contributions

$$f_m^\pm(n, k_z, s) = \frac{1}{2} [f_m(n, k_z, s) \pm f_m(n, \tilde{k}_z, s)] \quad (23)$$

that are even and odd with respect to the change of k_z by \tilde{k}_z where \tilde{k}_z belongs to the same valley and satisfies the equation $E_m(n, \tilde{k}_z, s) = E_m(n, k_z, s)$. Since the even contribution in Eq. (23) is in fact a function of the electron energy, it nullifies the elastic scattering integral

and also makes no contribution to the current. Introducing the momentum relaxation times $\tau_p^{(f,i)}$ we can present the photocurrent as

$$j = -e \sum_{n_f, n_i, k_z, s} \left[v_c(n_f, k_z, s) \tau_p^{(f)} - v_c(n_i, k_z, s) \tau_p^{(i)} \right] W_{cc}(n_f, n_i, k_z, s) \quad (24)$$

for optical transitions $(c, n_i, s) \rightarrow (c, n_f, s)$ between the conduction subbands and in a similar way for transitions between the valence subbands or for interband transitions, where n_f, n_i are the angular momentum components in the final and initial states. The transition rate is given by

$$W_{cc}(n_f, n_i, k_z, s) = \frac{2\pi}{\hbar} |V_{fi}|^2 f_c^0[E_c(n_i, k_z, s)] \delta[E_c(n_f, k_z, s) - E_c(n_i, k_z, s) - \hbar\omega].$$

Here f_c^0 is the equilibrium distribution function and we assume that in equilibrium the upper subband (c, n_f, s) is unoccupied.

In this section we take a chiral CN with the parameter $\nu = 1$, assume that the tube is n -doped and consider the intersubband photoexcitation of electrons from the lowest conduction subbands $(c, n = 0, s)$ to the first higher subbands $(c, n = 1, K)$ and $(c, n = -1, K')$ (see Fig. 2). In order to obtain compact analytical results we consider near-edge optical transitions with the light frequency ω satisfying the condition

$$|\hbar\omega - \Delta_{10}| \ll \Delta_{10}, \quad (25)$$

where Δ_{10} is the energy separation between the subbands $(c, 0, K)$ and $(c, 1, K)$ given by, see Eqs. (8,10),

$$\Delta_{10} = \frac{1}{2}(\Delta_1 - \Delta_0) = \frac{2\pi\gamma}{3L}.$$

In this case $|k_z| \ll |k_\perp|$ and one can use the approximate equations (9)–(12). Rewriting Eq. (9) in the form

$$E_c(n, k_z; K) = \frac{\Delta_n}{2} - \frac{m_n \beta_n^2}{2\hbar^2} + \frac{\hbar^2(k_z + \kappa_n)^2}{2m_n} \quad (26)$$

with $\kappa_n = m_n \beta_n / \hbar^2$ we conclude that \tilde{k}_z entering Eq. (23) equals to $-k_z - 2\kappa_n$. We ignore the small frequency region where the terms linear-in- k_z exceed or are comparable with the

quadratic terms in- k_z in Eq. (9) and assume the ratios $\alpha_n(k_z) = \beta_n k_z / (\hbar^2 k_z^2 / 2m_n)$ for $n = 0, 1$ to be small which is valid if

$$|k_z| \gg 2m_n \beta_n / \hbar^2 \text{ or } |\hbar\omega - \Delta_{10}| \gg 2m_n \beta_n^2 / \hbar^2.$$

Taking into account Eq. (17) and retaining the first-order terms in α_n we can write the photocurrent as a sum of four contributions

$$j_{CPGE} = eW_{1,0}(l_v + l_m + l_\tau + l_f). \quad (27)$$

Here $W_{1,0}$ is the transition probability rate per unit length calculated neglected the terms linear- k :

$$W_{1,0} = \frac{2\pi}{\hbar} \frac{2\pi e^2 I}{\omega^2 c n_\omega} \frac{1}{32} \left(\frac{\gamma}{\hbar} \frac{k_z}{k_{\perp,0}} \right)^2 f_c^0(E_0) g_{10}(\Delta_{10} - \hbar\omega), \quad (28)$$

I is the light intensity in units $energy \cdot length^{-1} \cdot time^{-1}$, the one-dimensional reduced density of states equals to

$$g_{10}(E) = 2 \times \sum_{k_z} \delta\left(-\frac{\hbar^2 k_z^2}{2\mu_{10}} - E\right) = \frac{1}{\pi} \left(\frac{2\mu_{10}}{\hbar^2 E} \right)^{1/2} \theta(-E),$$

the factor of two makes allowance for the spin degeneracy, $\theta(x)$ is the step function equal to 0 if $x < 0$ and 1 if $x > 0$, $-\mu_{10}^{-1}$ is the inverse reduced effective mass $m_1^{-1} - m_0^{-1}$, (since $m_1 = 2m_0 > m_0$ a value of $\mu_{10} = 2m_0$ is positive and $g_{10}(E)$ is defined for negative values of E), and $f_c^0(E_0)$ is the value of the equilibrium distribution function at the energy $E_0 = (\hbar^2 k_z^2 / 2m_0) = (\mu_{10} / m_0)(\Delta_{10} - \hbar\omega) = 2(\Delta_{10} - \hbar\omega)$. The lengths l_v, l_m, l_τ, l_f in Eq. (27) are related to the photoexcitation asymmetry arising due to the k_z -dependence of the velocity and density of states (l_v), of the squared matrix element (l_m), of the momentum relaxation time (l_τ) and of the equilibrium distribution function (l_f). For the optical transitions under consideration the straightforward derivation results in

$$l_v = \frac{3\beta_0}{\hbar} (\tau_p^{(1)} - \tau_p^{(0)}), \quad l_m = \frac{2\beta_0}{\hbar} (\tau_p^{(1)} - 2\tau_p^{(0)}), \quad (29)$$

$$l_\tau = \frac{6\beta_0}{\hbar} \left(\tau_p^{(1)} \frac{d \ln \tau_p^{(1)}}{d \ln E_1} - \tau_p^{(0)} \frac{d \ln \tau_p^{(0)}}{d \ln E_0} \right), \quad l_f = \frac{3\beta_0}{\hbar} (2\tau_p^{(0)} - \tau_p^{(1)}) \frac{\Delta_{10} - \hbar\omega}{k_B T} [1 - f_0(E_0)].$$

Obviously, the momentum relaxation time $\tau_p^{(1)}$ is shorter than $\tau_p^{(0)}$ because a photoelectron excited to the subband $((c, n = 1))$ can be readily scattered to the subband $((c, n = 0))$.

The circular photocurrent can be estimated as

$$j_{CPGE} \sim eW_{1,0} \frac{\beta_0}{\hbar} \tau_p P_{circ} \quad (30)$$

and for intensities at the absorption saturation

$$j_{CPGE} \sim \frac{2\pi \sin 3\theta}{\sqrt{3}} \frac{e}{\tau_p} \frac{a}{L} \left(\frac{\Delta_{10}}{\Delta_{10} - \hbar\omega} \right)^{1/2}.$$

Taking $\gamma = 6.5 \text{ eV}\cdot\text{\AA}$, $a = 2.5 \text{ \AA}$, $\nu = 1$, $L = 135 \text{ \AA}$, $\sin 3\theta = 0.7$ we have $\Delta_{10} = 0.1$, $m_0 = 0.017m$, where m is the bare electron mass, $\beta_0/\hbar = 1.1 \times 10^6 \text{ cm/s}$. Then for $\tau_p = 10^{-11} \text{ s}$, $\Delta_{10} - \hbar\omega = 0.1 \Delta_{10}$, and $f_c^0(E_0) \sim 1$ we obtain $j_{CPGE} \sim 10^{-9} \text{ A}$. While making this estimation we assumed the difference $\tau_p^{(0)} - \tau_p^{(1)}$ and the electron-electron scattering time τ_{ee} to be comparable with $\tau_p^{(0)}$. It is worth to mention that a value of the photocurrent in recently discovered crystals of CNs [31] will be significantly enhanced compared to a single CN.

We conclude the section by comparing the CPGE described by Eq. (30) with the photon drag (PD) effect which exists in crystals of arbitrary symmetry and is independent on the sign of the circular polarization. The PD current is estimated as

$$j_{PD} \sim eW_{1,0} \frac{\hbar q}{m_0} \tau_p, \quad (31)$$

where q is the photon wave vector (in vacuum $q = \omega/c$). Thus, for $\hbar\omega = 0.1 \text{ meV}$ we have $j_{CPGE}/j_{PD} \sim \beta_0 m_0 / (\hbar^2 q) \approx 3$.

In this section we presented both the detailed calculation and estimation by an order of magnitude for the CPGE. In the next chapters we restrict ourselves only to analytical estimations of other effects while their detailed consideration can be given elsewhere.

IV. MAGNETO-INDUCED LINEAR PHOTOGALVANIC EFFECT.

In addition to the circular PGE, in noncentrosymmetric media a photocurrent of another kind can be induced by the electro-magnetic wave. This is called the linear photogalvanic

effect (LPGE) and described by a third-rank tensor, χ_{ijk} , symmetrical with respect to the interchange of the indices j and k . Thus, for the LPGE one has [7]

$$j_{LPGE,i} = \chi_{ijl} I (e_j e_l^* + e_j^* e_l) / 2. \quad (32)$$

Ideal CNs are unpolar with their principal axis, z , being two-sided which forbids the photocurrent (32). In $B_x C_y N_z$ nanotubes (BNs) the symmetry is reduced, the axis z is polar and the LPGE becomes allowed [21]. We show here that the linear photocurrent can be induced in an ideal CN in the presence of an external magnetic field $\mathbf{B} \parallel z$. Phenomenologically the magneto-induced LPGE can be written as

$$j_{M-LPGE,z} = I B_z [\Lambda_{\parallel} |e_z|^2 + \Lambda_{\perp} (|e_x|^2 + |e_y|^2)] \quad (33)$$

and determined by two linearly independent coefficients $\Lambda_{\parallel}, \Lambda_{\perp}$.

For the interband transitions $(v, 0) \rightarrow (c, 0)$ excited in an undoped CN by the linearly polarized light, $\mathbf{e} \parallel z$, one has the following estimation

$$j_{M-LPGE,z} \sim e W_{0,0} \frac{\beta_0}{\hbar} \tau_p \nu \frac{\Phi}{\Phi_0}. \quad (34)$$

The estimation follows if we take into account the quadratic term in the expansion of h in powers of ka . Due to this term the squared matrix element of the optical transition has an odd contribution, the ratio of the odd contribution to the main even contribution being proportional to $ak_z \sin 3\theta$. In the magnetic field the band gaps $\Delta_{00}(K), \Delta_{00}(K')$ differ due to the difference of $|k_{\perp}|$ and $|k'_{\perp}|$ at $n = 0$ (See Eq. (13) and Fig.3 where the scheme of the optical transitions is shown. The different thickness of lines in Fig.3, which correspond to the transitions of electrons with different momenta indicate that they probabilities are different). This leads to the relative difference in the transition rates for the K and K' valleys proportional to

$$\frac{\Delta_{00}}{\hbar\omega - \Delta_{00}} \nu \frac{\Phi}{\Phi_0}.$$

Thus the linear magneto-photocurrent induced by the light polarized along the principal axis z can be estimated as

$$j_{M-LPGE,z} \sim eW_{0,0} ak_z \sin 3\theta \frac{\hbar k_z}{m_0} \frac{\Phi}{\Phi_0} \frac{\Delta_{00}}{\hbar\omega - \Delta_{00}} \tau_p.$$

Since

$$k_z \frac{\hbar k_z}{m_0} \sim \frac{\hbar\omega - \Delta_{00}}{\hbar}$$

and $\Delta_{00} \sim \gamma k_{\perp,0}$, $\beta_0 \sim a\gamma \sin 3\theta$ we obtain

$$j_{M-LPGE,z} \sim eW_{0,0} \frac{\Delta_{00}a}{\hbar} \tau_p \sin 3\theta \frac{\Phi}{\Phi_0}$$

and finally arrive at Eq. (34). The same order of magnitude for $j_{M-LPGE,z}$ is obtained if we ignore the quadratic terms in $h(\mathbf{k})$ but include the cubic- k_z terms in the energy dispersion Eq. (7). Above we assumed Φ to be much smaller than Φ_0 . For large values of Φ the linear magneto-photocurrent is a periodic function of the ratio Φ/Φ_0 . While preparing the manuscript we learned about a similar work [25] on the magneto-induced linear photovoltaic effect.

V. MAGNETO-INDUCED *dc* ELECTRIC CURRENT QUADRATIC IN THE ELECTRIC FIELD

Eq.(35) for magneto-induced linear PGE holds at high frequencies $\omega > \tau_p^{-1}$. This effect, however, does not vanish even in the case $\omega = 0$: the chiral symmetry allows existence of a current which is quadratic in the electric field and linear in the external magnetic field. In the case of bulk metals this effect has been observed in [28].

In the case of chiral CN a general expression for *dc* current has the form

$$j_z = \sigma E_z + \Lambda E_z^2 B_z, \tag{35}$$

where $\sigma = e^2 n \tau_p / m_0$ is the linear Drude conductivity, τ_p is the momentum relaxation time and m_0 is the effective mass in the lowest conduction subband, and we assume the Fermi level lies below the bottom of the subbands ($c, \pm 1$). Note that the magneto-chiral coefficient Λ is nonzero only in chiral CNs.

Qualitatively, the nature of the magneto-chiral correction can be understood as follows: the electric field accelerates electrons (in n -doped samples) and creates a nonequilibrium electron distribution. In this section we assume that the elastic electron relaxation rate is much larger than the inelastic one, which is associated with the electron-phonon scattering. Then in the first approximation in the ratio between these rates the electron distribution function depends only on the electron energy. It should be determined from the balance of the energy supplied to the electron system by the electric field and the energy transferred by electrons to the acoustic phonons. It is important that the distribution functions which depend only on the electron energy correspond to zero current. To get a nonzero value of the dc current we have to take into account that in the case of chiral CN the electron-phonon inelastic scattering rate depends on the direction of the electron momentum. As a result, there is a correction to the electron distribution function which is odd-in- k_z , the value of which is proportional to the ratio between the inelastic and elastic relaxation rates. In other words, the electron-phonon inelastic processes convert a currentless distribution of the electron gas into a distribution characterized by a nonzero electric current, proportional to E^2 .

An antisymmetric part of the probability rate for the electron inelastic scattering can be found if we use the symmetry considerations and write, in addition to the 2×2 Hamiltonian (3), the operator of the electron-phonon interaction for a graphene sheet near the point \mathbf{K}

$$V_{e-phon} = \begin{pmatrix} \Xi_0 u & \Xi u_+ \\ \Xi u_- & \Xi_0 u \end{pmatrix}. \quad (36)$$

Here $u = u_{11} + u_{22}$, $u_{\pm} = u_{11} - u_{22} \pm iu_{12}$, u_{lm} is the in-plane strain tensor in the axes x_1, x_2 and Ξ_0, Ξ are the deformation potential constants. In the tight-binding model $\Xi = -\Xi_0/2$. Let u_{zz} be a uniform strain in a single CN. Then the strain-induced shift of the electron energy in the subband $(c, 0)$ in the K valley is equal to

$$\varepsilon_u(\theta; K) = \left[\Xi_0 - \frac{\sqrt{3}}{2} \Xi \left(\frac{k_{\perp,0}}{k_0} \cos 3\theta + \frac{k_z}{k_0} \sin 3\theta \right) \right] u_{22} \quad (37)$$

and $\varepsilon_u(\theta; K') = \varepsilon_u(-\theta; K)$. Here $k_0 = \sqrt{k_{\perp,0}^2 + k_z^2}$. It follows from the above equation that

the ratio of the part odd-in- k_z to the part even-in- k_z for the rate of electron scattering by a phonon can be estimated as

$$\eta(k_z) \equiv \frac{W^{(-)}}{W^{(+)}} \sim \frac{k_z}{k_0} \sin 3\theta. \quad (38)$$

At zero magnetic field the asymmetry induced by inelastic processes in the k_z distribution in the valley K is compensated by the asymmetry in the K' valley and the quadratic-in- E_z current is zero. The magnetic field shifts the bottoms of the K and K' valleys relative to each other (See Eqs. (9,13)), the equilibrium electron densities in these valleys become different leading to a current contribution proportional to $E_z^2 B_z$.

In contrast to the previous consideration of free-standing CNs we consider here a CN that lies on a solid surface and is effected by 3D acoustic phonons of the solid. It allows to uncouple the momentum and energy conservation laws in electron-phonon scattering processes. Then the correction to the dc current proportional to $E^2 B_z$ is estimated as

$$\delta j_z \sim e \langle W^{(+)} \eta(\bar{k}_z) \zeta [\tau_p(k_{f,z}) v(k_{f,z}) - \tau_p(k_{i,z}) v(k_{i,z})] \rangle, \quad (39)$$

where δj_z is the part of the current proportional to E_z^2 ,

$$\zeta \sim \frac{\gamma k_{\perp,0}}{E_F} \frac{\Phi}{\Phi_0}, \quad (40)$$

is the relative difference of the electron equilibrium densities in the valleys K and K' induced by the magnetic field, see Eqs. (10,13), E_F is the Fermi energy referred to the conduction band bottom, τ_p is the momentum relaxation time, $v(k_z) = \hbar k_z / m^*$ is the electron velocity, $k_{f,z}$ and $k_{i,z}$ are the initial and final values of k_z in the inelastic scattering process, we assume the difference $k_{f,z} - k_{i,z}$ to be much smaller than $\bar{k}_z = (k_{f,z} + k_{i,z})/2$; the angle brackets mean the averaging over k_z . A value of $W^{(+)}$ is estimated from the balance of energy as

$$k_B T W^{(+)} = \sigma E_z^2, \quad (41)$$

where k_B is the Boltzmann's constant and we take into account that the typical electron energy change under scattering is of the order of the thermal energy or, analytically,

$$\hbar^2 \bar{k}_z (k_{i,z} - k_{f,z}) / m^* \sim k_B T .$$

Here we consider the degenerate electron gas and assume $k_B T$ to be much smaller than the Fermi energy E_F . Then Eq. (39) can be reduced to

$$\delta j_z \sim e \sigma E^2 \sin 3\theta \tau_p \frac{\gamma}{\hbar E_F} \frac{\Phi}{\Phi_0} \quad (42)$$

or

$$\frac{\delta j_z}{j_z} \sim \sin 3\theta \frac{e E \tau_p}{\hbar} \frac{\gamma}{E_F} \frac{\Phi}{\Phi_0} . \quad (43)$$

We would like to mention that in the approximation of purely elastic scattering δj_z is zero. Nevertheless Eqs. (42,43) is independent of inelastic scattering rate. This is because we considered the case when the sample length is larger than the inelastic diffusion length, $\sqrt{D_p \tau_{in}}$, where $D_p \sim v_F^2 \tau_p$ is the elastic diffusion coefficient and v_F is the Fermi velocity, and we used the equation (41). In the opposite limit the value of the current is proportional to τ_{in}^{-1} .

Assuming, for example, that the voltage bias on the sample is $U \sim 0.01V$, $E_F \sim 0.1eV$, $\tau_p \gamma / \hbar \sim L_{CN}$ and, hence, $E_z \tau_p \gamma / \hbar \sim U$, $\Phi / \Phi_0 \sim 10^{-2}$ (for $B_z = 10$ T, $L = 70$ Å), we get the estimate $\delta j_z / j_z \sim 10^{-3}$.

VI. CHIRALITY EFFECTS IN OPTICAL SPECTROSCOPY

In this section we present estimates for two other effects of chirality in optical spectroscopy of CNs: the natural circular dichroism and the magneto-chiral dichroism.

Let us start with the natural circular dichroism appearing as a difference in the interband or intersubband optical transition rates for the σ_+ and σ_- light polarizations. As mentioned above, in bulk semiconductors the theory of natural optical activity is based on allowance for coupling between the electron spin and wavevector. Contrary to the approach [18], we ignore the spin-orbit interaction in CNs because it is negligible for C atoms and take into account the coupling between the angular momentum n and the wavevector k_z . We assume

the circularly polarized light to propagate along the principal axis z of a chiral nanotube with $\nu = 1$ and consider the interband optical transitions $(v, 0, K) \rightarrow (c, 1, K)$, $(v, -1, K') \rightarrow (c, 0, K')$ allowed for the σ_+ polarization and $(v, 1, K) \rightarrow (c, 0, K)$, $(v, 0, K) \rightarrow (c, -1, K)$ allowed for the σ_- polarization. The energy conservation law reads $E_c(n_f, k_z + q; K) - E_v(n_i, k_z; K) = \hbar\omega$, $E_c(n_f, k'_z + q; K') - E_v(n_i, k'_z; K') = \hbar\omega$. Due to the presence of the light wavevector q in these equations and the linear-in- k_z terms in the energy dispersion given by Eq. (9), the absorption probability rates $W(\sigma_{\pm})$ for the σ_{\pm} polarization differ and the relative difference is given by

$$\frac{W(\sigma_+) - W(\sigma_-)}{W(\sigma_+) + W(\sigma_-)} \sim \frac{\beta q}{\hbar\omega - \Delta_{10}^{cv}}, \quad (44)$$

where Δ_{10}^{cv} is the band gap between $(c, 1, K)$ and $(v, 0, K)$ subbands. For comparison we present also an estimation for the circular dichroism due to the Faraday effect in the magnetic field $\mathbf{B} \parallel z$:

$$\frac{W(\sigma_+) - W(\sigma_-)}{W(\sigma_+) + W(\sigma_-)} \sim \frac{\Delta_{10}^{cv}}{\hbar\omega - \Delta_{10}^{cv}} \frac{\Phi}{\Phi_0}. \quad (45)$$

If the condition (19) is not satisfied the depolarization effect can substantially renormalize the dichroism, however the ratio of the relative differences given by Eqs. (44,45) holds unchanged.

Let us now turn to an estimate of the magnitude of the magneto-chiral dichroism which manifests itself in the dependence of the light absorption coefficient on the product $q_{\alpha} B_{\beta}$. Here q_{α} and B_{β} are components of the light wavevector \mathbf{q} and the magnetic field \mathbf{B} [22,23], (see also [24] and references therein). In chiral CNs the magneto-chiral dichroism can be described by the following contribution to the absorption or emission probability rate [24]

$$\delta W = B_z q_z [Q_{\parallel} |e_z|^2 + Q_{\perp} (|e_x|^2 + |e_y|^2)]. \quad (46)$$

For the interband transitions $(v, 0, s) \rightarrow (c, 0, s)$ ($s = K, K'$) one has $Q_{\parallel} \neq 0$, $Q_{\perp} = 0$ and $\delta W_{00} \propto B_z q_z |e_z|^2 = B_z \cos \theta_0 \sin^2 \theta_0$, where θ_0 is the angle between the nanotube axis z and the propagation direction of the light linearly polarized in the plane containing the

vector \mathbf{q}_0 and the axis z . For the transitions $(v, 0) \rightarrow (c, 0)$ in one valley, say the valley K , the ratio $\delta W_{00}/W_{00}$ is given by $\beta q_z/(\hbar\omega - \Delta_{00})$ similarly to the previous consideration. At zero magnetic field the transitions in the valley K' lead to a contribution to δW_{00} of the opposite sign and the net value of δW_{00} vanishes. An external magnetic field breaks the compensation, and the imbalance in contributions from the K and K' valleys is governed by a value of $[\Delta_{00}/(\hbar\omega - \Delta_{00})](\Phi/\Phi_0)$. As a result we obtain

$$\frac{\delta W_{00}}{W_{00}} \sim \frac{\beta q_z \Delta_{00}}{(\hbar\omega - \Delta_{00})^2} \frac{\Phi}{\Phi_0}. \quad (47)$$

VII. CONCLUSION

All chirality induced effects considered above are not specific for chiral CN. In principle they should be present in any mesoscopic system lacking the mirror-reflection symmetry. In particular they should be present in mesoscopic disordered metallic samples where all possible symmetries are broken. Some of these effects have been already discussed [29,30].

Another system where the effects considered above can manifest themselves is a DNA molecule, which electron transport properties have been investigated recently [26,27]. Although usually DNA have large resistance, we would like to mention in this connection that the photoinduced electron transport effects can be measured even in diamond [6].

The photogalvanic effects should also exist in Josephson junctions with no mirror-reflection symmetry. For example, it could be either superconductor-carbon nanotube-superconductor or superconductor-disordered metal-superconductor junctions. The qualitative difference of the photogalvanic effects in metals is that the circularly polarized light will induce both the normal and superfluid components of the current through the junctions.

The theory presented above neglects effects of electron-electron interaction including the excitonic and Luttinger-liquid effects. In this respect we would like to mention that Φ -dependent terms in the electron spectrum will suppress the dip in the energy dependence of the density of states for interacting electrons in one dimension [32]. In disordered samples

the magnitude of this effect should match results [33–35] for diffusive quasi-one-dimensional conductors.

Finally we would like to mention an effect which is inverse to the circular and linear photogalvanic effects. Namely, in the absence of magnetic field the dc electric current in a CN should induce the circular polarization of the photoluminescence. In the presence of an external magnetic field parallel to a CN, the electric current j_z should induce a change in the photoluminescence intensity proportional to $j_z B_z$.

The work of B.Spivak was supported by Division of Material Sciences, U.S. National science foundation under contract No. DMR-9205144. The work of E.L.Ivchenko was supported by programmes of Russian Academy and Ministry of Sciences. We would like to acknowledge useful discussions with D. Cobden, C. Kane, L. Levitov and C. Markus.

REFERENCES

- [1] S. Ijima, Nature (London), **354**, 56, (1991).
- [2] Physics World **13**, N.6, 2000.
- [3] S. Tasaki, K. Maekawa, and T. Yamabe, Phys. Rev. B **57**, 9301 (1998).
- [4] E.L. Ivchenko and G.E. Pikus, Zh. Exsp. Teor. Phys. Pis'ma **27**, 640 (1978) [JETP Lett. **28**, 74 (1978)].
- [5] V.I. Belinicher, Phys. Lett. A **66**, 213 (1978).
- [6] B.I. Sturman, V.M. Fridkin, The Photovoltaic and Photorefractive effects in Non-centrosymmetric Materials, Gordon and Breach Science Publishers, 1992.
- [7] E.L. Ivchenko and G.E. Pikus, Superlattices and Other Heterostructures. Symmetry and Optical Phenomena, Springer Series in Solid State Sciences, vol. 110, Springer-Verlag, 1995; second edition 1997; Ch. 10.
- [8] S. D. Ganichev, H. Ketterl, W. Prettl, E. L. Ivchenko, L. E. Vorobjev, Appl. Phys. Lett. **77**, 3146 (2000).
- [9] S. D. Ganichev, S. N. Danilov, V.V. Bel'kov, E. L. Ivchenko, H. Ketterl, L. E. Vorobjev, M. Bichler, W. Wegscheider, and W. Prettl, Physica E **10**, 52 (2001).
- [10] S. D. Ganichev, E. L. Ivchenko, S. N. Danilov, J. Eroms, W. Wegscheider, D. Weiss, and W. Prettl, Phys. Rev. Lett **86**, 4358 (2001).
- [11] H. Ajiki and T. Ando, J. Phys. Soc. Japan **62**, 1255 (1993); *ibid.* **62**, 2470 (1993); *ibid.* **64**, 4382 (1995).
- [12] H. Ajiki and T. Ando, Physica B **201**, 349 (1994).
- [13] H. Ajiki and T. Ando, J. Phys. Soc. Japan **65**, 505 (1996).
- [14] C.L. Kane and E.J. Mele, Phys. Rev. Lett **78**, 1932 (1997).

- [15] M.S. Dresselhaus, G. Dresselhaus, and R. Saito, Phys. Rev. B **45**, 6234 (1992).
- [16] R. Saito, M. Fujita, G. Dresselhaus, and M.S. Dresselhaus, Phys. Rev. B **46**, 1804 (1992).
- [17] C.T. White, D.H. Robertson, and J.W. Mintmire, Phys. Rev. B **47**, 5485 (1993).
- [18] E.L. Ivchenko and G.E. Pikus, Fiz. Tverd. Tela **16**, 1933 (1974).
- [19] A. Jorio, R. Saito, C.M. Lieber, M. Hunter, T. McClure, G. Dresselhaus, and M.S. Dresselhaus, Phys. Rev. Lett **86**, 1118 (2001).
- [20] E.L. Ivchenko, A.V. Selkin, and S.A. Permogorov, Solid State Commun. **28**, 345 (1978).
- [21] P. Král, E.J. Mele, D. Tománek, Phys. Rev. Lett. **85**, 1512 (2000).
- [22] E.F. Gross, B.P. Zakharchenya, and O.V. Konstantinov, Fiz. Tverd. Tela **3** 305 (1961).
- [23] E.L. Ivchenko, V.P. Kochereshko, G.V. Mikhailov, and I.N. Uraltsev, Phys. Stat. Sol. (b) **121**, 221 (1984).
- [24] G.L.J.A. Rikken and E. Raupach, Nature **390**, 493 (1997).
- [25] O. V. Kibis, Physica E **12**, 741, (2002).
- [26] A.Kasumov, M.Kociak, S.Gueron, B.Reulet, V.Volkov, D.Klinov, H.Bouchiat, Science. **291**, 280, 2001.
- [27] M.Kruger, M.R.Buitelaar, T.Nussbaumer, C.Schonenberger, Appl.Phys.Let. **78**, 1291, 2001.
- [28] G. L. J. A. Rikken, J. Flling, and P. Wyder Phys.Rev.Lett. **87**, 236602, 2002.
- [29] V.Falko, D.Khmelnitskii, Sov.Phys.JETP, **68**, 186, 1989.
- [30] B.Spivak, F.Zhou, M.T. Beal Monod, Phys.Rev. B **51**, 13226, 1995.
- [31] R.R.Schlitler, J.W. Seo, J.K.Gimzewski, C.Duncan, M.S.M. Saifullmah, M.E. Welland,

Science, 292, 1136, 2001.

[32] Marc Bockrath, David H. Cobden, Jia Lu, Andrew G. Rinzler, Richard E. Smalley, Leon Balents, and Paul L. McEuen, Nature 397, 598 (1999).

[33] B.L.Altshuler, A.G.Aronov, P.A.Lee, Phys.Rev.Lett. **44**, 1288, (1980).

[34] Yu. Nazarov, Sov.Phys.JETP, **68**, 561, (1968).

[35] S.Levitov, A.Shytov, JETP-Letters. **66**, 124, 1997;

FIGURES

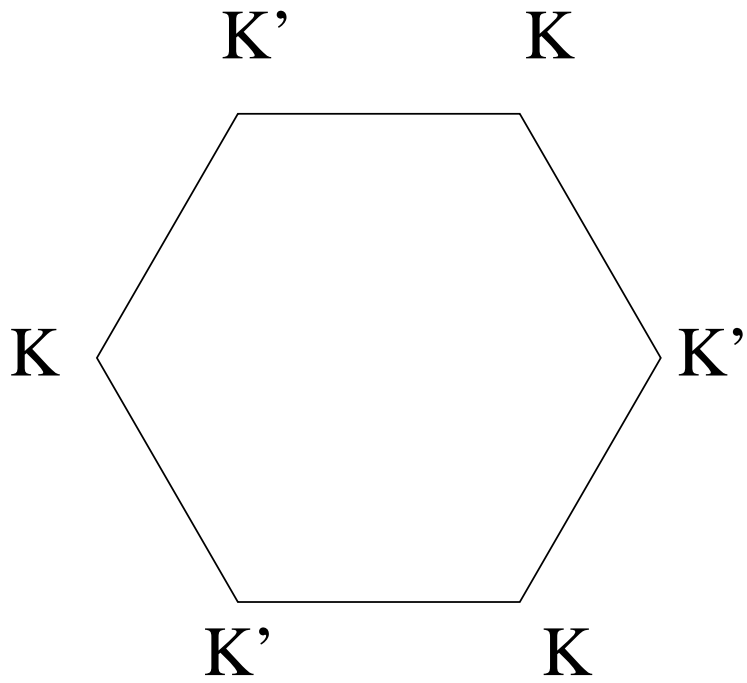


FIG. 1. Two dimensional Brillouin zone of graphene.

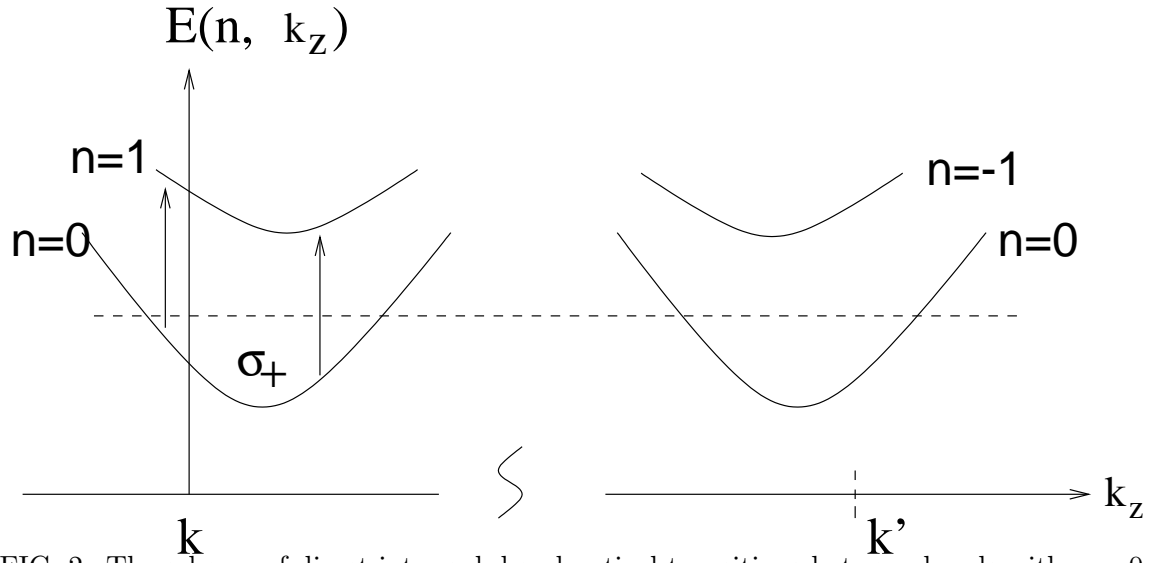


FIG. 2. The scheme of direct inter-sub-band optical transitions between bands with $n = 0$ and $n = 1$. The dashed line corresponds to the level of the chemical potential in the conduction band.

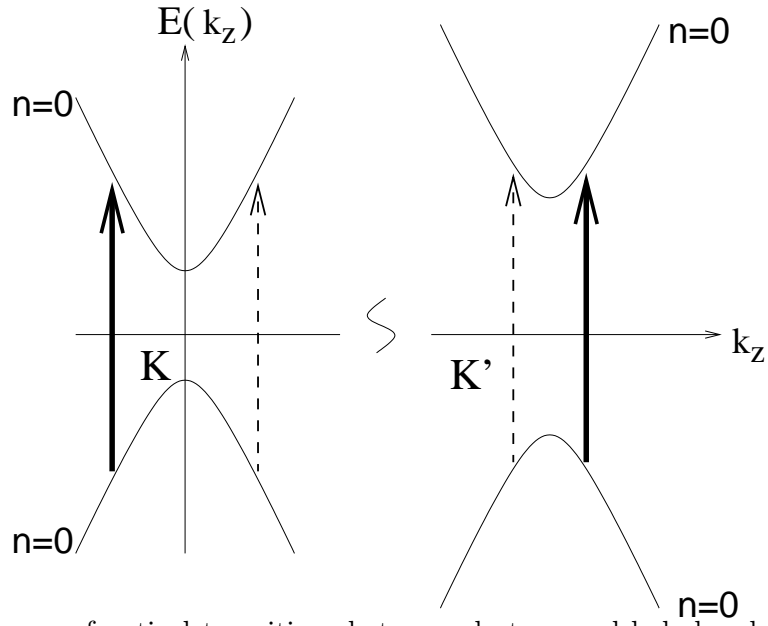


FIG. 3. A scheme of optical transitions between electron and hole bands with $n = 0$ in the case of linearly polarized light and in the presence of the external magnetic field. The dashed lines with different width correspond to transitions with different probabilities.